INES : 3D EDDY CURRENT IMAGING FOR A NONDESTRUCTIVE EVALUATION SYSTEM APPLIED TO STEAM GENERATOR TUBES

R. Zorgati*, V. Monebhurrun**, P.O. Gros*, B. Duchêne**,
D. Lesselier**, and C. Chavant*

* EDF - Research & Development Division,
6, quai Watier - BP 49 - 78401 Chatou, France
** CNRS-ESE - Plateau de Moulon
91192 Gif-sur-Yvette Cedex France

CONTEXT

Nuclear power plants supply about 80% of the total production of electricity in France. Non-Destructive Evaluation (NDE) is of prime importance in verifying the soundness of components such as the steam generator (SG), casted elbows, core, etc. In order to facilitate diagnostic, now mainly performed through signal processing and human interpretations, we attempt to image damaged internal structures of these components through data inversion. This NDE inverse approach, similar to medical imaging, was successfully applied to radiographic NDE of casted elbows. From a few number of projections (less than 10) and after rough localization of defects, our software SIROCCO3D is able to reconstruct 3D images of flaws using ART and markovian inverse algorithms [1].

The importance of the safe operation of SG is such that we have defined a project, named INES (Imaging for a Nondestructive Evaluation System), which aims to design and develop a similar system devoted to 3D Eddy Current (EC) imaging of SG tubes. These can be divided into four homogeneous areas : U-bend, support plate, straight part and roll expansion zone. Presently, our project is at a feasability stage and this paper considers first results obtained on simulated data related to the straight part of the tube. The characteristics of the probe, which have yet to be designed, are not taken into account here.

THE FORWARD PROBLEM

The first step consists in solving the forward problem i.e. evaluation of the anomalous field generated by a flaw with known electromagnetic characteristics. A mathematical model has to be established, thus enabling us to predict the signals which we will obtain through experiments. Validation of this model is simply done by comparing experimental and simulation data with some reasonable margin for errors. This process needs definition of suitable test-cases and thereby costly realization of specific mock-ups.

EC-NDE Configuration

The typical EC-NDE situation is described in Figure 1. The object to be inspected –a metal block– occupies domain D_2, which is inaccessible to measurement and is flawed by a defect occupying area Ω. An EC probe moved through air (D_1) collects the interaction between radiation, produced by an exciting source, and the object. In the inverse problem, this measured signal, characteristic of the soundness of the object, is processed in order to determine the parameters of the damaged zone. Defects are seen as a spatial modification of the electromagnetic parameters (conductivity and permeability) with respect to their standard values (for a sound metal). A crack is then supposed to be, from an electromagnetic point of view, a variation of conductivity whereas stress can be roughly modelled as a variation of permeability.

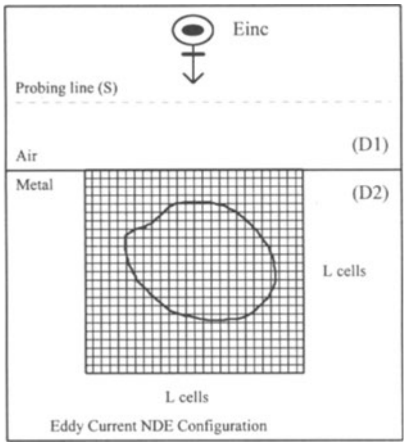

Figure 1 : EC-NDE configuration.

Formulation of the Problem

After applying Maxwell's equations, we obtain a Helmholtz equation:

$$\left[\Delta + k^2\right]\mathbf{U}(\vec{r}) = \mathbf{J}(\vec{r}) \tag{1}$$

where the possible expressions for the current density, **J**, with respect to the electrical formulation we choose and the type of defect we would like to treat, are given in the following table:

Table 1: Expression of the Current Density

J = J1 + J2 + J3			
	J1	**J2**	**J3**
Ω_σ	$(k_\sigma^2(\vec{r}) - k_0^2)\mathbf{E}(\vec{r})$	0	0
Ω_μ	$(k_\mu^2(\vec{r}) - k_0^2)\mathbf{E}(\vec{r})$	0	$\vec{\nabla}\mu(\vec{r}) \wedge \frac{1}{\mu(\vec{r})}\nabla \wedge \mathbf{E}(\vec{r})$
$\Omega_{\sigma\mu}$	$(k_{\sigma\mu}^2(\vec{r}) - k_0^2)\mathbf{E}(\vec{r})$	0	$\vec{\nabla}\mu(\vec{r}) \wedge \frac{1}{\mu(\vec{r})}\nabla \wedge \mathbf{E}(\vec{r})$

Solving with a Volume Integral Method

This integral formulation, well suited for inversion purposes, implies difficult computations of the Green's dyadic function which appears in the equations linking the electric fields to the flaw parameters. The coupling or state equation reads:

$$\mathbf{E}_2(\bar{\mathrm{r}}) = \mathbf{E}_2^{inc}(\bar{\mathrm{r}}) + \int_\Omega \overline{\overline{\mathbf{G}}}_{22}(\bar{\mathrm{r}}, \bar{\mathrm{r}}')\, \mathbf{J}(\bar{\mathrm{r}}')d\bar{\mathrm{r}}' \quad \text{where} \quad \mathbf{J}(\bar{\mathrm{r}}) = \left[\mathrm{k}^2(\bar{\mathrm{r}}) - \mathrm{k}_0^2\right]\mathbf{E}_2(\bar{\mathrm{r}}) \tag{2a}$$

$\mathbf{J}$ is the current density induced in the flaw zone, k the wave number, $\overline{\overline{\mathbf{G}}}$ the dyadic Green's function and $\mathbf{E}$ the electric field (by convention, index "1" relates to domain D_1, index "2" to domain 2 and the subscript "*inc*", valid for both media, relates to the situation in the absence of any flaw). The observation equation is similarly given by:

$$\mathbf{E}_1(\bar{\mathrm{r}}) = \mathbf{E}_1^{inc}(\bar{\mathrm{r}}) + \int_\Omega \overline{\overline{\mathbf{G}}}_{12}(\bar{\mathrm{r}}, \bar{\mathrm{r}}')\, \mathbf{J}(\bar{\mathrm{r}}')d\bar{\mathrm{r}}' \tag{2b}$$

During inspection of SG tubes, the response usually measured is the impedance change of the probe as it is moved along the axis of the tube. If I_0 is the current carried by the probe, the expression of the impedance variation is given by Auld's formula:

$$\Delta Z(\bar{r}) = \left(\frac{-1}{I_0^2}\right)\int_\Omega \mathbf{E}_2^{inc}(\bar{r}')\mathbf{J}(\bar{r}')d\bar{r}' \tag{3}$$

Computation of the Green's Dyadic Function

The detailed derivation of the Green's dyadic function is found in [2] but a general expression is given below. The 9 components of this dyad constitute the electric field response due to a point-source of electric current in a cylindrically stratified media. Each of the 3 independent polarizations of the source yields the 3 components of the electric field accordingly. A Dirac delta term appears in the expression to take into account the singularity of the Green's function:

$$\overline{\overline{\mathbf{G}}}ij \rightarrow \sum_{n=-\infty}^{\infty} \int_{-\infty}^{\infty} e^{jn(\phi-\phi')+jk_z(z-z')} \begin{bmatrix} G_{\rho\rho} & G_{\rho\phi} & G_{\rho z} \\ G_{\phi\rho} & G_{\phi\phi} & G_{\phi z} \\ G_{z\rho} & G_{z\phi} & G_{zz} \end{bmatrix} (\rho, \rho')dk_z - \frac{\delta(\mathrm{r}-\mathrm{r}')}{k_j^2}\hat{\rho}\hat{\rho} \tag{4}$$

Discrete Model

After discretization using a Method of Moments [3], the basic equations become a coupled system of linear matrix equations, where the unknowns that interest us (in the forward problem) are the vectors **y** and **b** , respectively the electric field distribution in the flaw and the response of the probe:

$$\begin{cases} \mathbf{G_1 X y = b} \\ \\ \mathbf{(I - G_2 X) y = d} \end{cases} \Leftrightarrow \begin{cases} \mathbf{G_1 Y x = b} \\ \\ \mathbf{(I - G_2 X) y = d} \end{cases} \tag{5a}$$

$$\mathbf{X} = diag(x = \sigma \ - \sigma_0),\ \mathbf{Y} = diag(y \ = e_2) \tag{5b}$$

$$\mathbf{b = e_1 - e_0^{\mathit{inc}} = G_1 X e_2 = G_1 X (I - G_2 X)^{-1} e_0^{\mathit{inc}}} \tag{5c}$$

A conjugate gradient scheme is then employed to solve for the electric field distribution. Only a few number of iterations is sufficient for a satisfactory convergence in our case.

Results

The probe consists in 2 axisymmetric coils placed close to each other and carrying counterflowing currents (differential-type probe). The incident electric field in the metal can be shown to have only one component, namely E_ϕ. This particularity of the field leads to some simplification of the problem already considered by Sabbagh [4]. It consists in neglecting any possible depolarization of the field in the flaw. This assumption helps to relieve the burden of computation with a full dyadic so that, in our case, only the $G_{\phi\phi}$ term of the dyad is needed when solving for the electric field in the flaw. Same numerical results as the exact solution to the problem have been obtained thereby confirming the validity of this approximation.

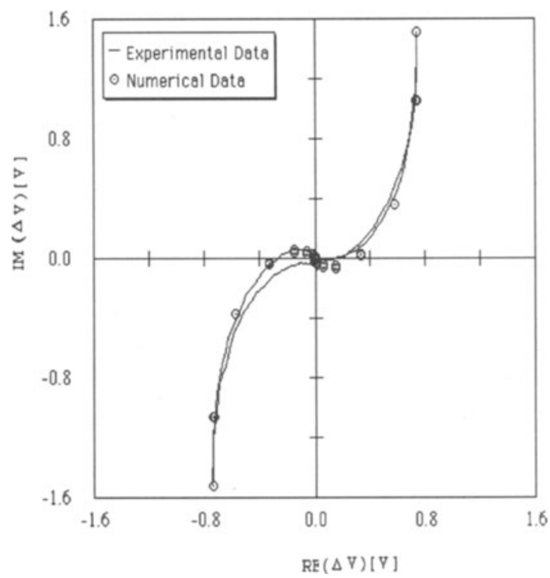

Figure 2 : Comparison of simulated and experimental data.

Figure 2 shows the comparison of simulated and experimental data obtained at 100 kHz in the case of a through-wall crack (depth= 1.27 mm (100 %) , diameter= 1.6 mm).

THE INVERSE PROBLEM

A usual SG tube flaw configuration, for example a 3D internal notch, is shown in Figure 3c. From a set of measurements y (Fig. 3a), the inverse procedure aims to reconstruct images of the defect x, via an inversion model (Fig. 3b). Comparison of reconstructed images of defects with their realistic mock-up counterparts is again essential for the validation of the inversion procedure.

The eddy current inverse problem has three main features which should be taken into account for the development of a suitable inversion algorithm: nonlinearity, ill-posedness and attenuation. Actually, it is extremely difficult to take into account all of these features to define a robust inversion algorithm. Our study will be focused only on inversion methods based on a nonlinear framework. Two different methods are presented: one based on the modified gradient approach [5] and the other known as the global generalized inverse method.

The Modified Gradient Method with Binary Constraint

This method is based on the conjugate gradient scheme with simultaneous search of the electric field and the contrast function, x. A binary specialization of this method has been studied by [6] in various domains of applications and is applied here.

- Step 1: define an *a priori* on the solution

We assume that the defect to be retrieved is a crack so that the contrast function is a binary function. However, our inversion scheme relies on the search of the contrast function along its gradient. So that, in order to restore differentability, we define a new function which takes the following form:

$$X(\vec{\mathbf{r}}) = \frac{1}{1 + e^{-\left(\frac{\tau(\vec{\mathbf{r}})}{\theta}\right)}} \tag{6a}$$

i.e. a function which depends continuously upon an auxiliary variable τ. The parameter θ plays the same role as the cooling parameter in the simulated annealing algorithm.

- Step 2: define the functional to optimize

The nonlinearity of the problem is taken into account by simultaneously minimizing a cost functional F defined via weighted residuals of the state and observation equations:

SIGNAL TO PROCESS	INVERSION MODEL	DEFECT TO RETRIEVE
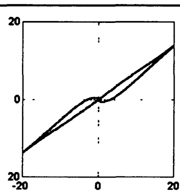	$G_1 E_2 x = y$ $(I - G_2 X) e_2 = e_2^{inc}$	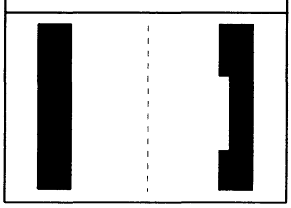
(3a)	(3b)	(3c)

Figure 3: The data (3a) and the model (3b) are used in order to retrieve the defect (3c).

$$F = \sum_{q=1}^{Nq} \left[\frac{1}{\left\| \mathbf{E}_{1q}^{inc} \right\|_S^2} \left\| \rho_q \right\|_S^2 + \frac{1}{\left\| \mathbf{E}_{2q}^{inc} \right\|_D^2} \left\| r_q \right\|_D^2 \right] \tag{6b}$$

where $r_q = \mathbf{E}_{2q} - \mathbf{E}_{2q}^{inc} - \mathbf{G}_{Dq} X \, \mathbf{E}_{2q}$ and $\rho_q = \mathbf{E}_{1q} - \mathbf{E}_{1q}^{inc} - \mathbf{G}_{Sq} X \, \mathbf{E}_{2q}$
and the index of summation q corresponds to the number of frequencies used (multifrequency reconstruction).

- Step 3: optimize the functional

We optimize simultaneously in E and X (through τ) using a conjugate gradient technique:

$$\mathbf{E}_{2q}^{n} = \mathbf{E}_{2q}^{(n-1)} + \alpha_q^n \mathbf{V}_q^n \tag{6c}$$

$$\tau^n = \tau^{(n-1)} + \beta^n \xi^n \tag{6d}$$

The reconstruction shown below is that of a crack of length=0.8 mm, width= 0.5° and depth=0.3 mm. As can be seen , this method yields a good image of the defect. However, because of the nonlinearity involved, the CPU time for the reconstruction is considerable (about 5 minutes on a Cray C94). It is interesting to notice that, due to attenuation in the metal, the deep parts of the defect are shadowed.

The Global Generalized Inverse Method

In contrast to the previous method, we attempt to solve for the unknowns by considering linear equations. The inversion procedure is as follows:

- Step 1: solve in current density

Writing the state equation in terms of current density leads to only one unknown which is solved using a conjugate gradient technique. An essential point to bear in mind is that the current density includes radiating and non-radiating sources [7]. The latter has to be evaluated through some convenient way but has not been considered here since it can be neglected in certain cases.

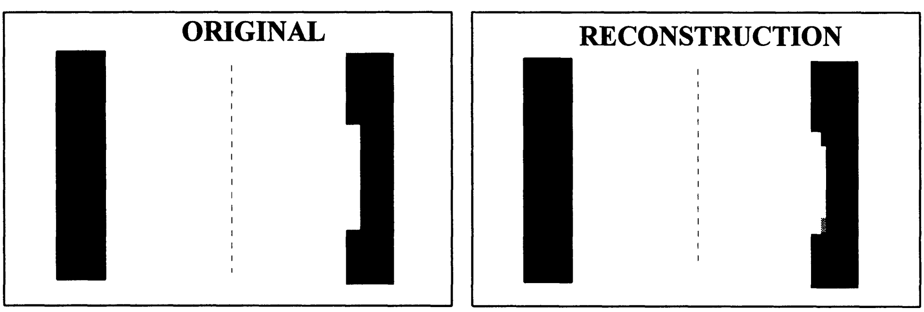

Figure 4 : Reconstruction of a crack with the modified gradient method.

$$\mathbf{E}_1(\vec{r}) = \mathbf{E}_1^{inc}(\vec{r}) + \int_\Omega \overline{\overline{\mathbf{G}}}_{12}(\vec{r}, \vec{r}\,')\, \mathbf{J}(\vec{r}\,')d\vec{r}\,'$$
$$\hat{\mathbf{j}} = (\mathbf{G}_{12})^{+}(\mathbf{e}_1 - \mathbf{e}_1^{inc}) \tag{7a}$$

- Step 2: evaluate the internal field

From the estimate of the current density above, we evaluate the electric field distribution from the coupling equation:

$$\mathbf{E}_2(\vec{r}) = \mathbf{E}_2^{inc}(\vec{r}) + \int_\Omega \overline{\overline{\mathbf{G}}}_{22}(\vec{r}, \vec{r}\,')\, \mathbf{J}(\vec{r}\,')d\vec{r}\,'$$
$$\hat{\mathbf{e}}_2 = \mathbf{e}_2^{inc} + \mathbf{G}_{22}\hat{\mathbf{j}} \tag{7b}$$

- Step 3 : solve for the contrast function

Finally, since the electrical field is now estimated, the observation equation contains only x as unknown. A conjugate gradient scheme is again applied to solve for the contrast function defined as previously with a binary constraint:

$$\mathbf{E}_1(\vec{r}) = \mathbf{E}_1^{inc}(\vec{r}) + \int_\Omega \overline{\overline{\mathbf{G}}}_{12}(\vec{r}, \vec{r}\,')\, X(\vec{r}\,')\mathbf{E}_2(\vec{r}\,')d\vec{r}\,'$$
$$\hat{x} = \left[\mathbf{G}_{12}\, diag(\hat{\mathbf{e}}_2)\right]^{+}(\mathbf{e}_1 - \mathbf{e}_1^{inc}) \tag{7c}$$

The figure below shows the reconstruction of the same flaw considered before. The result is as good as the modified gradient method but the algorithm is much faster (about a few seconds). The effect of neglecting non-radiating sources is currently being studied in different flaw configurations.

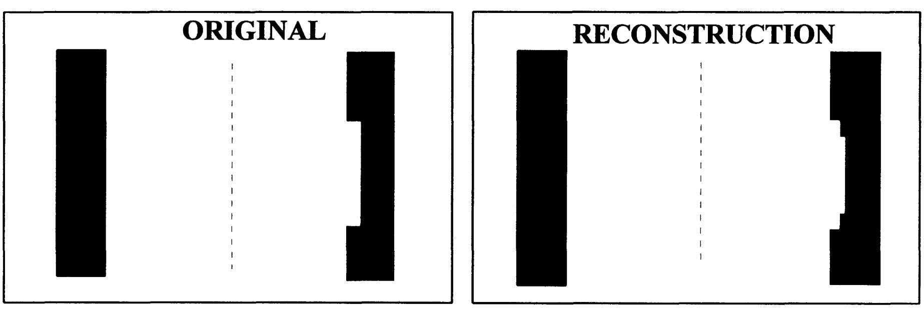

Figure 5: Recontruction of a crack with the global generalized inverse method.

CONCLUSION

In order to facilitate diagnostic, a project named INES has been defined with the aim to design a 3D imaging system for SG tubes. To evaluate the feasability of our project and to point out the main problems to be overcome, we focused on a simplified, but fully 3D, situation: straight part of a tube and academic probe.

The forward problem has been solved with a volume integral method and validated by comparison with experimental data. Amongst the several inversion techniques studied, two of them have been presented here, namely the modified gradient algorithm and the global generalized inverse method. Regarding the results obtained, eddy current imaging seems indeed possible, although the present inversion techniques do not simultaneously take into account nonlinearity, attenuation and ill-posedness.

However, an overall solution to these three issues has to be found for the development of a robust and efficient algorithm for real EC data inversion. In addition, to complete our imaging system, a suitable probe needs to be designed and the study extended to the roll expansion, plate zones and U-bend.

AKNOWLEDGEMENTS

The authors would like to extend sincere thanks to Mr TESSA of the CMS Compagny, France, for his help in providing experimental signals on an ACME tube.

REFERENCES

1. B. Lavayssière, E. Fleuet and B. Georgel, "3D reconstruction: A Challenge in Non-Destructive Testing", 2nd International Symposium on Inverse Problems, 2-4 Nov. 94, ISIP'94, Paris, France, pp 41-45, H. D. Bui *et al.* Ed., Balkema books, Rotterdam.
2. W. C. Chew, "Waves and Fields in Inhomogeneous Media", Dudley Ed., IEEE Press, 1995.
3. R. F. Harrington, "The Method of Moments in Electromagnetics", J. Electromagn. Waves Appli., Vol. 1, N°3, pp 181-200, 1987.
4. L. D. Sabbagh and H. A. Sabbagh, "Eddy-Current Modeling and Flaw Reconstruction", J. Nondestructive Evaluation, Vol. 7, N°12, pp 95-108, 1988.
5. R. E. Kleinman and P. M. Van den Berg, "A Modified Gradient Method for Two-Dimensional Problems in Tomography ", J. Comput. Appl. Math., Vol. 42, pp 17-35, 1992.
6. L. Souriau, B. Duchêne, D. Lesselier and R. E. Kleinman, "Modified Gradient Approach in Inverse Scattering for Binary Objects in Stratified Media", Inverse Problems, Vol. 12, pp 463-481, 1996.
7. T. Habashy, E. Chow, D. Dudley, "Profile Inversion Using the Renormalized Source-Type Integral Equation Approach," IEEE Trans. Antennas Propagat., Vol. 38, N°5, pp. 668-680, 1990.